

Formation of monocarboxylic acids and polyols on a graphite surface

C. Mendoza^{a,*}, L.S. Rodríguez^b, F. Ruetter^b, S. Schnell^c

^a Centro de Física, Instituto Venezolano de Investigaciones Científicas (IVIC), P.O. Box 21827, Caracas 1020A, Venezuela

^b Centro de Química, Instituto Venezolano de Investigaciones Científicas (IVIC), P.O. Box 21827, Caracas 1020A, Venezuela

^c Indiana University School of Informatics and Biocomplexity Institute, 1900 East Tenth Street, Eigenmann Hall 906, Bloomington, IN 47406, USA

Received 19 June 2007; accepted for publication 26 December 2007

Available online 1 January 2008

Abstract

A heterocatalytic model involving the graphite surface, which has been previously used for the surface formation of chemisorbed amino acids, is consistently extended to the synthesis of monocarboxylic acids and polyhydroxylated compounds. Extensive computations with semi-empirical and *ab initio* quantum chemical methods have been carried out to analyze reaction pathways on surface models of different sizes. The model assumes surface recombinations involving small functional groups. Polymerization is initiated by either a carboxyl (COOH) or a formyl (HCO) group that is anchored to the graphite surface through two chemisorption sites, and proceeds by the addition of mobile diffusors of the type CH_n ($1 \leq n \leq 3$) and $\text{CH}_{n'}\text{OH}$ ($0 \leq n' \leq 2$). Polymer length is determined by the competition between surface diffusion and hydrogenation. Some of the features observed in the laboratory regarding the surface self-assembly of monocarboxylic chains, in the organic inventory of star-forming regions and in carbonaceous meteorites can be addressed with the present approach.

© 2007 Elsevier B.V. All rights reserved.

Keywords: *Ab initio* quantum chemical methods and calculations; Semi-empirical models and model calculations; Models of surface chemistry reactions; Chemisorption; Compound formation; Organic molecules; Graphite

1. Introduction

The catalytic capabilities of a model graphite surface in the synthesis of simple amino acids have been previously studied with quantum chemical methods [1]. It is found that chemisorbed species can be built up from adsorbate–adsorbate (a–a) and adsorbate–free (a–f) surface processes in a hydrogen-rich environment where the surface essentially acts as a template. We report here calculations that show that such mechanisms can be consistently extended to the surface formation of monocarboxylic acids and polyhydroxylated compounds (polyols) such as sugars, sugar alcohols and sugar acids.

The surface formation of organic molecules is of interest in astrochemistry due to the observation of simple organic

acids and sugars in star-forming regions (hot molecular cores). Both acetic acid (CH_3COOH) [2] and glycolaldehyde (CH_2OHCHO) [3] have been detected in the Sgr B2 Large Molecule Heimat (LMH). An origin for these molecule in grain-surface chemistry has been suggested as a result of their association with other complex organic grain products, and it is speculated that the assembly of functional groups on the grain surface accounts for the high degree of isomerism displayed. The subsequent detection in the LMH of ethylene glycol ($\text{HOCH}_2\text{CH}_2\text{OH}$), the reduced alcohol of glycolaldehyde, hints again at a low-temperature chemistry on the grain surface or ice mantles [4], and the presence of aldehydes such as propynal (HC_2CHO), propenal (CH_2CHCHO) and propanal ($\text{CH}_3\text{CH}_2\text{CHO}$) [5] constitutes strong evidence for reaction pathways based on successive hydrogenations.

Carbonaceous chondritic meteorites, e.g. Murchison, Murray and Orgueil, have traditionally been rich sources of organic compounds such as sugars, sugar alcohols, sugar

* Corresponding author. Tel.: +58 212 5041533; fax: +58 212 5041148.
E-mail addresses: claudio@ivic.ve (C. Mendoza), fruetter@ivic.ve (F. Ruetter), schnell@indiana.edu (S. Schnell).

mono-acids and di-acids and deoxysugar acids [6]. Mono-carboxylic acids have been quantified in both straight- and branched-chain isomers in concentrations that decrease with increasing number of carbon atoms, the signature that supports extraterrestrial abiotic synthesis [7]. Aliphatic carboxylic acids with straight and branched chains of up to 12 and 9 carbon atoms, respectively, have also been identified in carbonaceous chondrites found in Antarctica in concentrations that decrease logarithmically with carbon number and display a high level of isomerism throughout [8].

Scanning tunnelling microscopy (STM) has been a powerful technique for laboratory studies of the properties of chemisorbed self-assembled monolayers which have technological applications in multiple fields [9]. In the case of organic thin films, STM has been hampered by image recognition, but the two-dimensional ordering of straight-chain hydrocarbons is being resolved. For instance, it has been found that carboxylic esters physisorb as linear chains on the surface of highly oriented pyrolytic graphite (HOPG) with the plane of the carbon skeleton parallel to the surface, a different geometry from that displayed in the gas phase [10–12]. The HOPG surface has also been used for the template-directed assembly of proteins, where it is found that the threefold symmetry of the graphite template is reproduced in the adsorbate assembly [13].

A current difficulty in molecular electronics is the mastering of the molecule–electrode bond, particularly in the case of metal electrodes. A promising alternative is to use a single-walled carbon nanotube (SWNT) covalently attached to an organic molecular bridge, e.g. amine end groups connected to carboxylic acid chains [14]. Furthermore, the SWNT capacitance is sensitive to surface adsorbates, an effect that can be used for the construction of high-performance sorption-based sensors by thinly coating the SWNT with chemoselective material [15].

Motivated by such diverse interest in organic surface chemistry, and following earlier work [1], we study the formation of organic species on a model graphite surface starting from simple functional groups. Since we are concerned with fairly large molecular structures and an extensive number of reaction routes, our computational strategy involves the use of both *ab initio* and semi-empirical quantum chemical methods. Apart from its effectiveness, this approach also leads to useful validations and accuracy estimates of the underlying physical chemistry. In Section 2 the graphite surface models and the numerical methods are described, followed by an analysis in Section 3 of the surface chemistry of functional groups in a hydrogen-rich environment. The syntheses of monocarboxylic acid chains and polyols are developed in Sections 4 and 5, and our findings are discussed in Section 6.

2. Surface models and numerical methods

Active surfaces are assumed to be of finite and variable size, an important problem being the dependency of reac-

tion pathways on surface model size. As shown in Fig. 1, three graphite surface models are considered: PAH1, a coronene molecule ($C_{36}H_{12}$); PAH2, circumcoronene ($C_{54}H_{18}$); and PAH3, circumcircumcoronene ($C_{96}H_{24}$). In the optimization of the adsorbate–substrate system, substrate relaxation is taken into account, and the surface chemisorption sites of interest are on top of a carbon atom, to be referred hereafter as site A, and on the bridge between two carbon atoms, site B [16,17]. Surface chemistry is assumed to occur via Langmuir–Hinshelwood adsorbate–adsorbate (a–a) and Eley–Rideal adsorbate–free (a–f) recombinations. The graphite surface model has been chosen in the present work for its simplicity, general interest in different fields and for the lack of reliable experimental data on surface composition and configurations, particularly in the astrophysical context.

The numerical strategy we have adopted is to use a relatively fast semi-empirical method, namely *CATIVIC* [18], to map out reaction routes which are then validated at a higher computational cost with the *ab initio* *GAUSSIAN 98* package [19]. *CATIVIC* is a second-generation, semi-empirical, quantum chemical package based on parametric Hamiltonians within the *MINDO/3* scheme of separating atomic and diatomic parameters [20], the parametric functional components of the total energy being similar to those in the *MINDO/SR* implementation [21]. It offers a powerful graphic user interface for molecular building and for displaying geometrical optimization routes. Data obtained with this method are referred to hereafter as *CAT*. Computations with *GAUSSIAN 98* are carried out in a density-functional-theory mode (*B3LYP*) with the bases 3-21G (hereafter *GA1*) and 6-31G** (hereafter *GA2*). In 3-21G two-basis functions are used to represent each valence atomic orbital while 6-31G** uses polarization basis sets.

Experimental data for formic and acetic acids are employed to benchmark these two numerical methods. For formic acid, it may be seen in Table 1 that *GA1* and *GA2* reproduce the experimental bond lengths and angles to better than 5%. *CAT* can also account for bond lengths to this accuracy, but differences as large as 11% are found for some bond angles. The *CAT* heat of formation agrees with experiment to better than 5%, perhaps due to the fact that the functional parameters for small organic molecules in *CATIVIC* are optimized with this quantity. The *GA1* value, on the other hand, differs from experiment by 30% but is improved to 12% in *GA2* at a notably higher computational cost. A similar situation is found for acetic acid (Table 2) where the measured bond lengths and angles are reproduced by all three methods to better than 4% while the *GA1* heat of formation is again poor. In spite of the higher accuracy of *GA2*, its computational cost makes it impractical to study surface processes on the relatively large surface models that are being considered in this work. Therefore, *CATIVIC* results will be hereafter validated with *GA1*. These comparisons indicate that the accuracy of computed energies is not entirely reliable. On the other hand, a useful measure of bond strength is the Wiberg

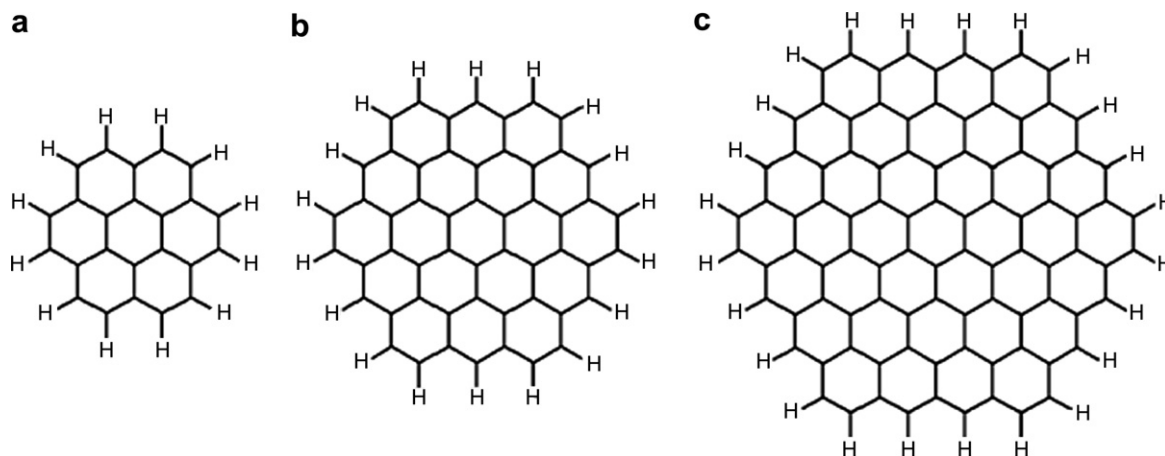


Fig. 1. Graphite surface models used in the present calculation. (a) PAH1: coronene ($C_{36}H_{12}$). (b) PAH2: circumcoronene ($C_{54}H_{18}$). (c) PAH3: circumcircumcoronene ($C_{96}H_{24}$).

Table 1
Data comparison for formic acid

	Expt.	CAT	GA1	GA2
$d(C^1O^1)$	1.202	1.203	1.220	1.227
$d(C^1O^2)$	1.343	1.321	1.375	1.372
$d(O^2H)$	0.972	0.950	1.000	0.984
$d(C^1H)$	1.097	1.137	1.093	1.091
$\angle(O^1C^1H)$	124.1	123.2	127.0	125.8
$\angle(C^1O^2H)$	106.3	118.0	108.9	111.3
$\angle(O^1C^1O^2)$	124.9	134.2	125.1	125.0
ΔH_f	-90.6	-86.8	-67.3	-101.8

Bond distances (d) in Å, angles in degrees and heat of formation (ΔH_f) in Kcal/mol. Experiment by Refs. [22,23].

Table 2
Data comparison for acetic acid

	Expt.	CAT	GA1	GA2
$d(C^1C^2)$	1.520	1.495	1.509	1.507
$d(C^1O^1)$	1.214	1.214	1.224	1.210
$d(C^1O^2)$	1.364	1.335	1.386	1.358
$d(C^2H)$	1.100	1.111	1.089	1.089
$\angle(C^2C^1O^1)$	126.6	124.3	128.0	126.1
$\angle(C^2C^1O^2)$	110.6	106.3	109.5	111.4
ΔH_f	-103.4	-104.8	-58.6	-96.2

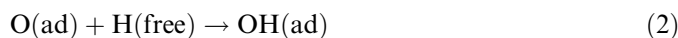
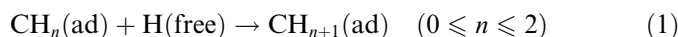
Bond distances (d) in Å, angles in degrees and heat of formation (ΔH_f) in Kcal/mol. Experiment by Refs. [22,23].

index computed by CATIVIC which is a quantity close to the bond order.

3. Surface functional groups

We have studied the formation of organic molecules on graphite model surfaces via a–a and a–f recombinations that involve simple functional groups of the type HCO, COOH, COH, CHOH, CH_2OH , CH, CH_2 and CH_3 . They can be generated as products of basic surface reactions starting from chemisorbed atomic C and O that get pro-

gressively hydrogenated and thus become more diffusive. For instance,



In the interstellar medium, they can also be produced by UV photolysis or proton irradiation of grain ice mantles rich in H_2O , CO, CH_3OH and CH_4 [24,25].

The three issues to consider are reactivity, surface diffusion and hydrogenation. We find by calculation that the relevant surface chemistry is mostly driven by reactions involving radicals. When the adsorbate has a dangling bond, e.g. CH_n ($1 \leq n \leq 2$) or CH_nOH ($0 \leq n' \leq 1$), it usually remains chemisorbed after a–a or a–f recombinations which in most cases are devoid of activation barriers. For fully coordinated adsorbates, CH_3 and CH_2OH say, reaction with a second adsorbate implies bond substitution and thus detachment from the surface which depends on the chemisorption energy. It has been found by calculation that CH_3 and CH_2OH only chemisorb at site A with CAT Wiberg indices of 0.91 and 0.87, respectively, that are practically independent of surface model size. Therefore, surface diffusion for these two adsorbates is limited to thermal hopping whereby the chemical bond with the surface must be broken before displacement occurs. In Table 3

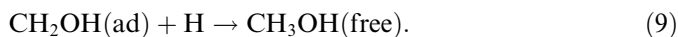
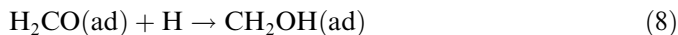
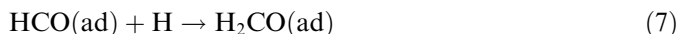
Table 3
Chemisorption energies (eV) for CH_3 and CH_2OH

	CAT		GA1	
	PAH1	PAH2	PAH1	PAH3
CH_3	-0.699	-0.255	-0.382	-0.395
CH_2OH	+0.047	-0.333	-0.460	-0.462

we list their chemisorption energies obtained with the different surface models; it may be seen that the GA1 energies (E_A) are within $-0.5 \leq E_A \leq -0.2$ eV and increase somewhat with surface size while CAT gives energies that are significantly different from GA1. By contrast, CH_n ($1 \leq n \leq 2$) and CH_nOH ($0 \leq n' \leq 1$) chemisorb at both A and B sites, and therefore surface diffusion may take place without desorption. In Table 4 the chemisorption energy differences between sites A and B, $\Delta E_{AB} \equiv E_A - E_B$, are given. For GA1, ΔE_{AB} is not larger than 0.7 eV except for CH, and it decreases with surface size. The CAT absolute values are noticeably smaller than those for GA1. It may be noticed that in Tables 3,4 the CAT chemisorption energies for PAH2 and PAH3 are not listed; this is due to unreliable values when the larger surface models are used which are caused by inaccurate functionals in CATIVIC at large interatomic distances.

Chemisorption of the carboxylic group (COOH), as well as that of formyl (HCO), occurs in three modes (see Fig. 2): through both the C and O atoms, i.e. two-site chemisorption (mode M1); via the O atom alone (mode M2) and through the C atom (mode M3). Wiberg indices are given as an indication of bond strengths. It may be seen that the uncoordinated C atomic component in M2 is too high (3.3 Å above the surface level) for a–a reactions to occur, and M3 is fully coordinated due to the double C=O bond. Hence, M1 is the only adsorbate configuration of COOH (and of HCO) of interest in surface reactions because of its accessible and uncoordinated C component; furthermore, since M1 is doubly chemisorbed, it is not likely to diffuse and acts as a receptor for mobile adsorbates in polymerization.

In H-rich environments (hot molecular cores, for instance, display H_2 number densities in the range 10^{12} – 10^{14} m^{-3} and temperatures of 100–300 K), hydrogenation competes with surface diffusion limiting the size of the molecular synthesis end-products. If it dominates, step-by-step hydrogenation of the CH_n and C_nOH adsorbates ultimately leads to desorbed methane (CH_4) and methanol (CH_3OH), respectively. Hydrogenation of the formyl adsorbate in the M2 and M3 modes (i.e. singly chemisorbed through its O and C components, respectively) produces free formaldehyde (H_2CO) in a single step while in the case of M1 (two-site chemisorbed) it follows the progression:



Similarly, in the case of the carboxylic M2 and M3 modes, a single hydrogenation yields free formic acid (HCOOH) while for M1 it takes the reaction route (see Fig. 3)

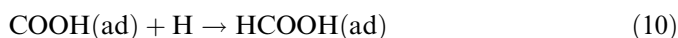
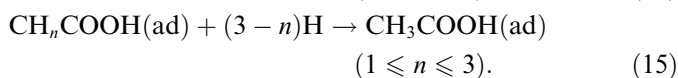
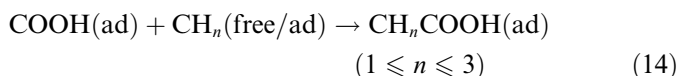


Fig. 3a–b show that the Wiberg index (I_w) gives an indication of which bond is likely to be replaced by hydrogenation. In Fig. 3a, the weakest bond is that of the O atom to the surface ($I_w = 0.79$), and in Fig. 3b it is one of the two C–O bonds ($I_w = 0.79$). Although free $\text{CH}_2(\text{OH})_2$ (methanediol) can be produced in the final reaction step (12), the free radical CHOH can also be liberated which is bound to react with a neighboring adsorbate causing further processing, e.g. vinyl alcohol



4. Monocarboxylic acid chains

When the surface reaction rates become comparable to or greater than hydrogenation, the graphite surface becomes a fertile ground for organic synthesis. In the case of monocarboxylic chains, reaction pathways start with the carboxylic M1 adsorbate (see Fig. 2) which initiates polymerization by taking the role of a fixed receptor for mobile CH_n diffusors. The smallest two-carbon chain, namely acetic acid (CH_3COOH), is thus formed in reaction pathways of the type



In the case of an a–a recombination with $n \leq 2$ in reaction (14), the CH_n fragment remains bonded to both the substrate and the COOH with similar bond strengths, $I_w \approx 0.91$ (see Fig. 4a). It is found by calculation that while the CH_n bond to the COOH adsorbate is always maintained during hydrogenation, the CH_n bond to the surface is broken during the last step ($n \rightarrow 3$) detaching it from the surface thus impeding further polymerization. The final chemisorbed configuration of acetic acid is depicted in Fig. 4b, and as listed in Table 5, its geometry is found to be insensitive to surface model size. A comparison of data by CAT and GA1 indicates that bond lengths and bond angles are probably accurate to within 5% and 10%, respectively. Reactions (14) and (15) can be alternatively initiated by a formyl M1 adsorbate yielding acetaldehyde (CH_3CHO).

Table 4
Differences in chemisorption energies (eV) between sites A and B (ΔE_{AB}) for different adsorbate–substrate systems

	CAT		GA1	
	PAH1	PAH1	PAH2	PAH3
CH	–0.910	–1.585	–0.957	–0.744
CH_2	0.119	0.340	0.279	0.003
COH	0.315	0.443	0.055	
HCOH	0.533	0.617	0.553	0.357

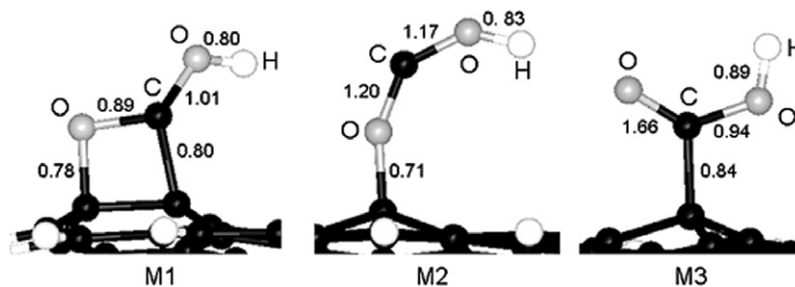


Fig. 2. Chemisorption modes of COOH on the graphite surface. For each bond, the Wiberg index is given as a measure of its strength. Due to the C=O double bond in M3 and the considerable height of the C atom in M2 (3.3 Å above the surface level), it is expected that only mode M1, through its low and uncoordinated C atom, will take part in productive a–a reactions.

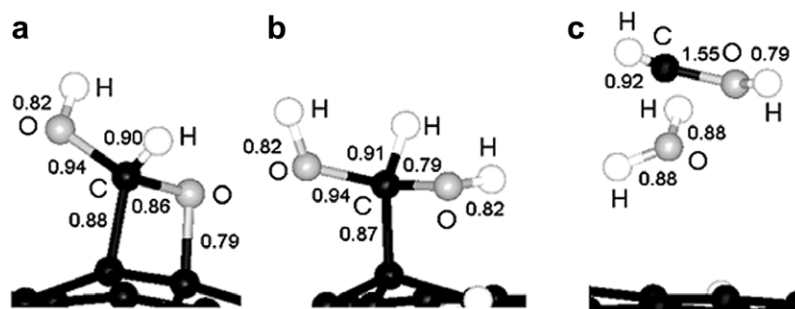


Fig. 3. Successive hydrogenations of chemisorbed COOH. Wiberg indices are given as measures of bond strengths. (a) Chemisorbed formic acid, HCOOH(ad). (b) HOCHOH(ad). (c) CHOH(free) + H₂O(free).

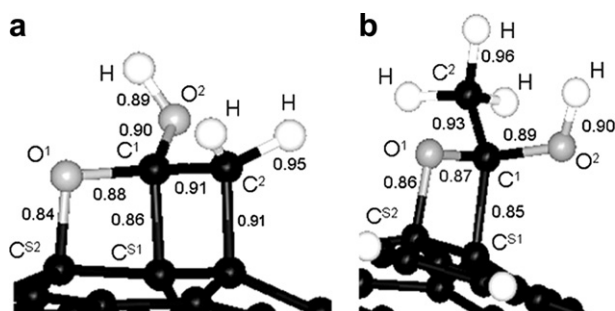
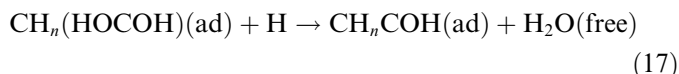
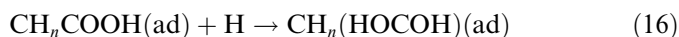


Fig. 4. Two-step formation of acetic acid on the graphite plane. (a) COOH(ad) + CH₂(ad). (b) CH₂COOH(ad) + H. It may be seen that the acetic acid adsorbate remains chemisorbed.

Successive hydrogenations of the COOH fragment within the CH_nCOOH adsorbate, instead of CH_n as shown in reaction (15), can also take place following a series of steps similar to those in reactions (11) and (12), namely



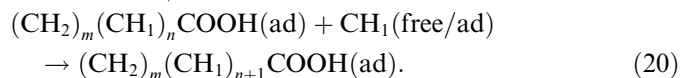
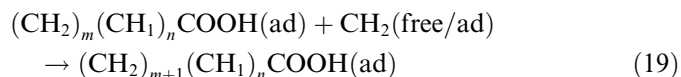
The option with $n = 2$ in step (18) is equivalent to chemisorbed vinyl alcohol while a further hydrogenation step with $n = 3$ produces free ethanol (CH₃CH₂OH).

If hydrogenation is much slower, further surface chemistry takes place leading to chain growth

Table 5
Computed geometry for chemisorbed acetic acid

	CAT		GA1	
	PAH1	PAH2	PAH1	PAH2
$d(\text{O}^1\text{C}^{\text{S}2})$	1.40	1.40	1.51	1.52
$d(\text{C}^1\text{C}^{\text{S}1})$	1.61	1.62	1.64	1.64
$d(\text{C}^1\text{O}^1)$	1.40	1.40	1.50	1.50
$d(\text{C}^{\text{S}1}\text{C}^{\text{S}2})$	1.61	1.60	1.57	1.56
$d(\text{C}^1\text{O}^2)$	1.37	1.37	1.40	1.40
$d(\text{O}^2\text{H})$	0.95	0.95	0.99	1.00
$d(\text{C}^1\text{C}^2)$	1.53	1.53	1.51	1.51
$d(\text{C}^2\text{H})$	1.11	1.11	1.09	1.09
$\angle(\text{C}^1\text{O}^1\text{C}^{\text{S}2})$	98.8	98.9	93.1	93.0
$\angle(\text{O}^1\text{C}^1\text{C}^{\text{S}1})$	88.9	88.7	89.4	89.2
$\angle(\text{C}^1\text{C}^{\text{S}1}\text{C}^{\text{S}2})$	82.8	83.0	86.0	86.2
$\angle(\text{C}^{\text{S}1}\text{C}^1\text{O}^2)$	104.5	104.5	116.8	116.9
$\angle(\text{C}^2\text{C}^1\text{O}^2)$	108.1	107.9	107.8	107.7
$\angle(\text{C}^2\text{C}^1\text{O}^1)$	109.4	109.3	111.5	111.3
$\angle(\text{C}^1\text{O}^2\text{H})$	116.1	116.1	108.2	108.9
$\angle(\text{C}^2\text{C}^1\text{C}^{\text{S}1})$	127.3	127.6	118.1	118.1
$\angle(\text{O}^1\text{C}^1\text{O}^2)$	119.1	119.7	112.2	112.6

Atomic labels as in Fig. 4b. Bond distances (d) in Å and angles in degrees.



In Fig. 5 we show the formation of a four-carbon chain with $m = 2$ and $n = 0$, i.e. solely built up from CH₂ monomers. It may be seen that the chain always remains

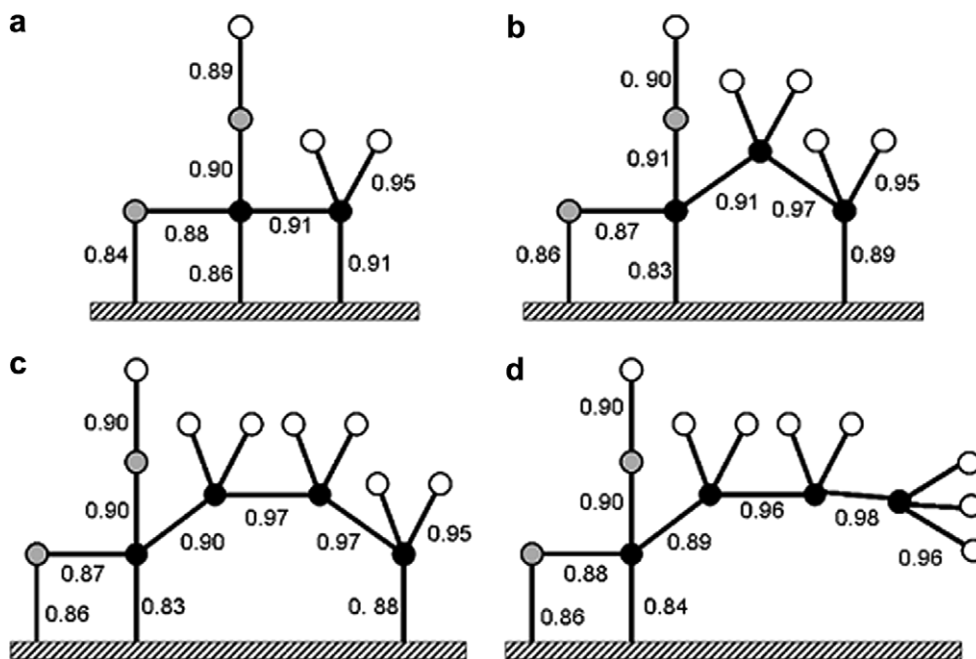
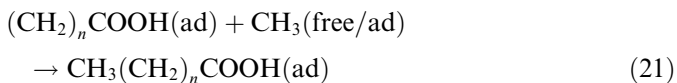
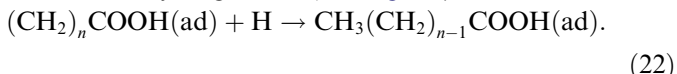


Fig. 5. Formation of a four-carbon monocarboxylic chain from a–a recombinations involving CH_2 diffusors on the graphite plane. Carbon atoms are depicted as black filled circles, oxygen as gray and hydrogen as white. Wiberg indices are given as measures of bond strengths. (a) Two-carbon chain. (b) Three-carbon chain. (c) Four-carbon chain. (d) Four-carbon chain with a saturated end monomer. Unless saturated, the tail end always remains adsorbed to the surface through the CH_2 end monomer thus enabling further polymerization.

chemisorbed through both the carboxylic head and the CH_2 tail end; moreover, the bond strengths of the former do not weaken during polymerization. The tail end is open to further polymerization unless it separates from the surface by reacting with a CH_3 monomer



or becomes hydrogenated (see Fig. 5d)



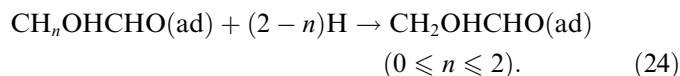
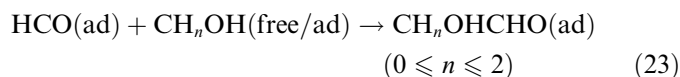
A relevant point is that a chain buildup only with CH_2 monomers, $n = 0$, gives rise to the straight-chain isomer while if CH diffusors are involved, $n > 0$, branching can occur. In contrast to CH_2 , CH remains bonded to the surface during chain assembling thus creating a bifurcation point for a second branch of surface reactions.

Polymerization in Eqs. (19) and (20) can be alternatively seeded by HCO instead of COOH . For instance, a chemisorbed species of the 3-C propanal molecule (CH_2CHCHO) can be formed in a two-step process involving reaction (20) with $m = n = 0$ and (19) with $m = 0$ and $n = 1$. Similarly, chemisorbed propanal ($\text{CH}_3\text{CH}_2\text{CHO}$) is produced by two reactions (19), the first with $m = n = 0$ and the second with $m = 1$ and $n = 0$, followed by hydrogenation of the end monomer.

5. Polyol formation

The formation of sugars, sugar acids and alcohols is similar to that described for monocarboxylic acids in

Section 4. It is found by calculation that polymerization is initiated by either the formyl or carboxylic group in the M1 two-site chemisorption mode (see Fig. 2), and is built up from diffusive adsorbates of the type CH_nOH ($0 \leq n \leq 2$). Polymer length depends again on the competition between surface diffusion and hydrogenation rates. For instance, the simplest two-carbon monosaccharide glycolaldehyde (CH_2OHCHO) can be formed in the two-step process



As expected, the resulting adsorbate configuration, as shown in Fig. 6, is similar to that of acetic acid, and its geometry (see Table 6) is again practically independent of

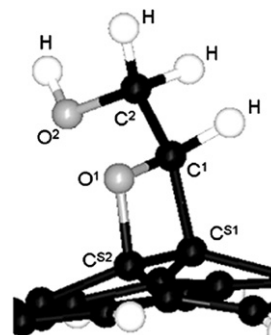


Fig. 6. Glycolaldehyde molecule chemisorbed on the graphite plane.

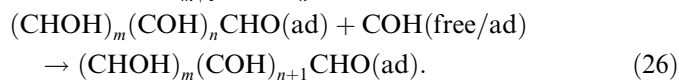
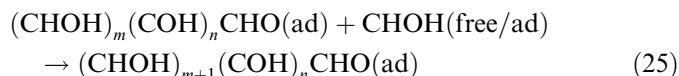
Table 6
Computed geometry for chemisorbed glycolaldehyde

	CAT		GA1	
	PAH1	PAH2	PAH1	PAH2
$d(\text{O}^1\text{C}^{\text{S}2})$	1.40	1.41	1.59	1.53
$d(\text{C}^1\text{C}^{\text{S}1})$	1.59	1.60	1.59	1.58
$d(\text{C}^1\text{O}^1)$	1.38	1.38	1.51	1.51
$d(\text{C}^{\text{S}1}\text{C}^{\text{S}2})$	1.61	1.58	1.57	1.57
$d(\text{C}^1\text{H})$	1.14	1.14	1.09	1.09
$d(\text{C}^1\text{C}^2)$	1.53	1.53	1.53	1.52
$d(\text{C}^2\text{O}^2)$	1.35	1.35	1.45	1.46
$d(\text{C}^2\text{H})$	1.13	1.13	1.09	1.09
$d(\text{O}^2\text{H})$	0.95	0.95	1.00	1.00
$\angle(\text{C}^1\text{O}^1\text{C}^{\text{S}2})$	97.6	97.9	91.0	91.0
$\angle(\text{O}^1\text{C}^1\text{C}^{\text{S}1})$	90.9	89.5	91.1	91.1
$\angle(\text{C}^1\text{C}^{\text{S}1}\text{C}^{\text{S}2})$	82.0	82.5	87.0	86.8
$\angle(\text{C}^{\text{S}1}\text{C}^1\text{H})$	109.5	107.8	111.5	113.1
$\angle(\text{C}^2\text{C}^1\text{H})$	100.6	101.8	112.6	111.4
$\angle(\text{C}^2\text{C}^1\text{C}^{\text{S}1})$	129.4	128.0	119.9	121.3
$\angle(\text{C}^2\text{C}^1\text{O}^1)$	115.8	117.8	108.2	106.7
$\angle(\text{C}^1\text{C}^2\text{O}^2)$	113.5	123.8	109.8	105.4
$\angle(\text{C}^2\text{O}^2\text{H})$	111.5	114.4	102.7	103.5
$\angle(\text{O}^1\text{C}^1\text{H})$	110.7	111.8	111.5	111.0

Atomic labels as in Fig. 6. Bond distances (d) in Å and angles in degrees.

surface model size. The CAT bond lengths are consistently smaller than GA1 (by 3%) while the bond angles are somewhat larger but they agree to within 10% and 15%, respectively. If two additional hydrogenation steps are considered in reaction (24), free ethylene glycol ($\text{HOCH}_2\text{CH}_2\text{OH}$) is produced.

If the hydrogenation step (24) is delayed, further polymerization is promoted by surface reactions of the type



Sugar alcohols (e.g. glycerol) can be generated in reaction (25) with $n = 0$ and $1 \leq m \leq 4$, desorbing after a threefold hydrogenation of the end monomers. Sugar acids (e.g. glyceric acid) are formed in reaction (25) if the HCO initiator is replaced by COOH, with $n = 0$ and $1 \leq m \leq 4$ and a single terminal hydrogenation. In the dicarboxylic sugar acid variant, polymerization with $n = 0$ and $2 \leq m \leq 4$ is brought to a halt by a second chemisorbed carboxyl group. The deoxy sugar acids, on the other hand, include a mixture of diffusors of the type CHO, CH_2 and CH_3COH .

6. Summary and discussion

Extensive quantum chemical calculations have been carried out to study the heterocatalytic capabilities of the graphite surface in the synthesis of carboxylic acid chains and polyols. Surface recombinations involve small functional groups, and it has been shown within the present model that molecular complexity depends on the dominance of surface diffusion over hydrogenation.

Polymerization is initiated by either a carboxyl (COOH) or a formyl (HCO) group anchored to the surface through two chemisorption sites, and grows with mobile diffusors of the type CH_n ($1 \leq n \leq 3$) and CH_nOH ($0 \leq n' \leq 2$). In the case of monocarboxylic acid chains, CH_n diffusors with $n = 2$ give rise to the straight-chain isomer while the involvement of those with $n = 1$ leads to branching. Polymerization is terminated by a CH_3 monomer or by detachment of the tail end from the surface due to hydrogenation.

Sugar polymerization relies on CH_nOH diffusors. A notable feature particular to sugar chains is that they display hydrogen bridge bonds that tend to increase curvature once the tail end is separated from the surface after hydrogenation. Moreover, further hydrogenations of the COOH or HCO polymer heads lead to the formation of alcohols.

The proposed surface recombination pathways have been validated by both semi-empirical and *ab initio* methods and by considering surface models of growing size. This latter aspect is shown to have some influence on chemisorption energies and diffusion barriers, particularly related to the extent of substrate reconstruction during adsorbate–substrate bonding. On the other hand, the determination of a more complete set of kinetic parameters that would allow dynamical estimates of the speeds of these reaction pathways would imply lengthier calculations (e.g. transition states and frequency factors) and the introduction of additional numerical approaches. Furthermore, current lack of measurements for data validation would also compromise the reliability of such estimates.

With regards to carboxylic acid surface polymerization, it is found, in agreement with experiment [10], that chains grow parallel to the surface. Since they are chemisorbed through their COOH heads, desorption would then be the result of the competition between the two surface bonds and the formation of the C=O double bond. It is also shown that both straight- and branched-chain isomers can be formed. Since both types have been detected in chondritic meteorites [7,8], this finding emphasizes the importance of measuring their relative concentrations as it would provide indications of the relative abundances and mobilities of the CH and CH_2 diffusors. Also, the observed logarithmic abundance decrease with increasing carbon number in the meteoritic chains appears to fit the proposed stepwise surface polymerization.

Present results allow inferences which may be of astrochemical interest. For instance, we show that for surface diffusion to take place on a graphite surface, relatively high surface temperatures ($T \geq 100$ K) are required to overcome energy barriers, and diffusion rates should in principle increase with surface temperature. This finding is of arguable relevance in the explanation of the observations of complex saturated organic molecules in the interstellar medium which are exclusively attributed to hot molecular cores, and in the increase in abundances for most species with grain temperature [26,27]. Although the present scheme can account for the synthesis of a large number of observed $\text{C}_x\text{O}_y\text{H}_z$ molecules, there are many that do

not fit its requirements. The most eminent case is methyl formate which is apparently formed by channels that do not involve a–a recombinations. Its relatively high abundance can then be interpreted as a measure of the slowness of a–a recombinations relative to hydrogenations. Further studies of the surface chemistry of methyl formate are currently in progress encouraged by the poor performance of gas-phase reactions in reproducing the observed abundances [28].

Acknowledgements

We are grateful to Professor Philip K. Maini (Centre for Mathematical Biology, University of Oxford, UK) for reading the manuscript and for helpful comments; and to Dr. Morella Sánchez (IVIC) for assistance with the computation of the heat of formation in the different codes. This project is partially funded by FONACIT, Venezuela, under Contract No. G-97000667.

References

- [1] C. Mendoza, F. Ruetter, G. Martorell, L.S. Rodríguez, *Astrophys. J.* 601 (2004) L59.
- [2] D.M. Mehringer, L.E. Snyder, Y. Miao, F.J. Lovas, *Astrophys. J.* 480 (1997) L71.
- [3] J.M. Hollis, F.J. Lovas, P.R. Jewell, *Astrophys. J.* 540 (2000) L107.
- [4] J.M. Hollis, F.J. Lovas, P.R. Jewell, L.H. Coudert, *Astrophys. J.* 571 (2002) L59.
- [5] J.M. Hollis, P.R. Jewell, F.J. Lovas, A. Remijan, H. Møllendal, *Astrophys. J.* 610 (2004) L21.
- [6] G. Cooper, N. Kimmich, W. Belisle, J. Sarinana, K. Brabham, L. Garrel, *Nature* 414 (2001) 879.
- [7] J.G. Lawless, G.U. Yuen, *Nature* 282 (1979) 396.
- [8] H. Naraoka, A. Shimoyama, K. Harada, *Orig. Life Evol. Biosph.* 29 (1999) 187.
- [9] R.K. Smith, P.A. Lewis, P.S. Weiss, *Prog. Surf. Sci.* 75 (2004) 1.
- [10] F. Tao, Y. Cai, S.L. Bernasek, *Langmuir* 21 (2005) 1269.
- [11] F. Tao, J. Goswami, S.L. Bernasek, *J. Phys. Chem. B* 110 (2006) 4199.
- [12] A.K. Bickerstaffe, N.P. Cheah, S.M. Clarke, J.E. Parker, A. Perdigon, L. Messe, A. Inaba, *J. Phys. Chem. B* 110 (2006) 5570.
- [13] C.L. Brown, I.A. Aksay, D.A. Saville, M.H. Hecht, *J. Am. Chem. Soc.* 124 (2002) 6846.
- [14] X. Guo et al., *Science* 311 (2006) 356.
- [15] E.S. Snow, F.K. Perkins, E.J. Houser, S.C. Badescu, T.L. Reinecke, *Science* 307 (2005) 1942.
- [16] C. Mendoza, F. Ruetter, *Catalysis Lett.* 3 (1989) 89.
- [17] T. Fromherz, C. Mendoza, F. Ruetter, *Mon. Not. R. Astron. Soc.* 263 (1993) 851.
- [18] F. Ruetter, M. Sánchez, G. Martorell, C. González, R. Añez, A. Sierraalta, L. Rincón, C. Mendoza, *Int. J. Quant. Chem.* 96 (2004) 321.
- [19] M.J. Frisch, et al., *Gaussian Inc.*, Pittsburg PA, 2002.
- [20] M.J.S. Dewar, D.H. Lo, *J. Am. Chem. Soc.* 93 (1971) 7201.
- [21] G. Blyholder, J. Head, F. Ruetter, *Theor. Chim. Acta* 60 (1982) 429.
- [22] D.R. Lide, *CRC Handbook of Chemistry and Physics*, 77th ed., CRC Press, Cleveland, Ohio, 1996.
- [23] J. Cioslowski, M. Schimeczek, G. Liu, V. Stoyanov, *J. Chem. Phys.* 113 (2000) 9377.
- [24] B.T. Draine, *Annu. Rev. Astron. Astrophys.* 41 (2003) 241.
- [25] E.L. Gibb, D.C.B. Whittet, A.C.A. Boogert, A.G.G.M. Tielens, *Astrophys. J. Suppl. Ser.* 151 (2004) 35.
- [26] M. Ikeda, M. Ohishi, A. Nummelin, J.E. Dickens, P. Bergman, Å. Hjalmarson, W.M. Irvine, *Astrophys. J.* 560 (2001) 792.
- [27] S.-Y. Liu, D.M. Mehringer, L.E. Snyder, *Astrophys. J.* 552 (2001) 654.
- [28] A. Horn, H. Møllendal, O. Sekiguchi, E. Uggerud, H. Roberts, E. Herbst, A.A. Viggiano, T.D. Fridgen, *Astrophys. J.* 611 (2004) 605.